



HAL
open science

Fast and direct analysis of oxidation levels of oil-in-water emulsions using ATR-FTIR

Samar Daoud, Elias Bou-Maroun, Laurence Dujourdy, Gustav Waschatko,
Nils Billecke, Philippe Cayot

► **To cite this version:**

Samar Daoud, Elias Bou-Maroun, Laurence Dujourdy, Gustav Waschatko, Nils Billecke, et al.. Fast and direct analysis of oxidation levels of oil-in-water emulsions using ATR-FTIR. Food Chemistry, 2019, 293, pp.307-314. 10.1016/j.foodchem.2019.05.005 . hal-02173332

HAL Id: hal-02173332

<https://u-bourgogne.hal.science/hal-02173332>

Submitted on 22 Jun 2020

HAL is a multi-disciplinary open access archive for the deposit and dissemination of scientific research documents, whether they are published or not. The documents may come from teaching and research institutions in France or abroad, or from public or private research centers.

L'archive ouverte pluridisciplinaire **HAL**, est destinée au dépôt et à la diffusion de documents scientifiques de niveau recherche, publiés ou non, émanant des établissements d'enseignement et de recherche français ou étrangers, des laboratoires publics ou privés.

Fast and direct analysis of oxidation levels of oil-in-water emulsions using ATR-FTIR

Published in: *Food Chemistry* **293** (2019) 307–314

Samar DAOUD^{*1}, Elias BOU-MAROUN¹, Laurence DUJOURDY², Gustav WASCHATKO³, Nils BILLECKE³ & **Philippe CAYOT**¹

¹ PCAV team, Unité mixte “Procédés alimentaires et microbiologiques”. AgroSup Dijon et Université Bourgogne Franche-Comté, PAM UMR A 02.102, F-21000 Dijon, France

² Service d’Appui à la recherche, AgroSup Dijon, F-21000 Dijon, France

³ Cargill R&D Centre Europe BVBA Havenstraat 84. B-1800 Vilvoorde, Belgium

* corresponding author: Samar Daoud, E-mail: samar.daoud@u-bourgogne.fr

Highlights

- Attenuated total reflection-Fourier transform infrared (ATR-FTIR) monitors lipid oxidation in oil-in-water (o/w) emulsions without lipid extraction
- Correlate spectral changes to conjugated diene values using partial least squares regression (PLSR) models
- Fast extraction of lipids to measure oxidation using peroxide value (PV), conjugated diene (CD) value, and thiobarbituric acid reactive substances (TBARs) in oil-in-water emulsions

ABSTRACT

Oxidation of omega-3 fatty acids is a major limitation on its enrichment in food and beverages. An efficient and simple method to monitor lipid oxidation in complex systems is essential to limit lipid oxidation during formulation and processing. Fish oil-in-water emulsions (20% v/v) were exposed to iron or free radical initiated oxidation. Conjugated dienes (CDs) were rapidly measured using a previously developed fat extraction method. Fourier transform infrared (FTIR) spectroscopy has been used to directly record chemical changes occurring during oxidation. Variations were noticed in different spectral regions despite the presence of broad water bands near 3400 and 1640 cm^{-1} . Partial least squares regression (PLSR) revealed correlations between CD values and full FTIR spectra (4000–600 cm^{-1}), and different spectral regions (e.g., 1800–1500 cm^{-1} , 1500–900 cm^{-1}). These correlations confirm that FTIR spectroscopy is a rapid and simple method for measuring lipid oxidation in complex foods without prior fat extraction.

Keywords :

- Lipid oxidation
- Oil-in-water emulsions
- Infrared spectroscopy
- Chemometrics
- Iron
- Radical initiator
- Fish oil

1. Introduction

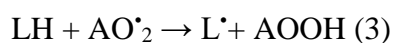
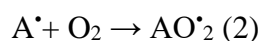
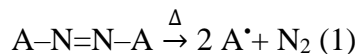
Consumption of ω -3 polyunsaturated fatty acids (PUFAs) is linked to improved human health. PUFAs play an important role during the development of the nervous system and in preventing cardiovascular diseases. While fish contains huge amounts of ω -3 PUFAs, increasing dietary fish consumption failed to provide the recommended levels of ω -3 fatty acids. Thus, functional food, containing ω -3 lipids, became one of the fastest growing food product categories in the US and Europe. A prerequisite for successful development of foods enriched with ω -3 PUFAs is the prevention of lipid oxidation (Walker et al., 2015). Lipid oxidation leads to product degradation, off-flavors, and other sensory alterations, which reduces consumer acceptance. Some lipid oxidation products are toxic for humans. The research enabling safe omega-3-product developments need fast and simple analytical tools.

Formulated foods often contain a lipid phase dispersed in an aqueous medium. Thus, they can be described as oil-in-water (o/w) emulsions (milk, cream, mayonnaise, sauces, and dressings). Hence, monitoring lipid oxidation in o/w emulsions is of great interest. The mechanism of o/w oxidation is more complicated than oxidation in bulk oil. The oil–water interface is a place where both water- and oil-soluble prooxidants and antioxidants can interact. An accurate and rapid analytical method to assess oxidation directly in emulsion is urgently required.

Infrared spectroscopy is based on the interaction between electromagnetic radiation and material. Energy absorbance depends on the molecules' functional groups; thus, qualitative and quantitative determination of organic compounds can be achieved. Fourier transform infrared (FTIR) spectroscopy is well known as a fast, nondestructive, and simple analysis that does not require sample preparation or use of organic solvents. Recent developments in FTIR spectroscopy resulted in an increase of its application for edible oil and fat analysis. It has been used to determinate fatty acid composition (Kim et al., 2007), perform adulteration studies (Vlachos et al., 2006), and measure lipid oxidation in bulk oil (Borchman & Sinha, 2002; Klaypradit et al., 2011; Lerma-García et al., 2011; Setiowaty & Che Man, 2003). The close relationships between specific infrared bands and lipid oxidation have been proved for a broad range of edible oils, such as sesame, sunflower, corn, soybean, and olive oils (Guillen & Cabo, 2000). Several predictions of oxidation markers (e.g., PV (Klaypradit et al., 2011), TBARs (Setiowaty & Che Man, 2003), and p-anisidine value (Klaypradit et al., 2011)) were accomplished when applying multivariate analysis such as PLSR on FTIR spectroscopy data. Although there are many reports on bulk oil oxidation, only a few studies analyzed oil

oxidations in emulsions, despite its importance for food applications (BELHAJ et al., 2010; Guzun-Cojocararu et al., 2011; Hayati et al., 2005; Nalur & Decker, 1994). These emulsion oxidation studies depend on a fat extraction step prior to analysis. Fat extraction is time-consuming. Thus, the standard methods (CD, PV, and p-Anisidine value for example) cannot be done simultaneously with the spectroscopic measurement, which makes it impossible to correlate the extracted molecules and their spectroscopic signal. Moreover, the extraction process can introduce errors in the determination of degree of oxidation when it is not done consistently and efficiently (Coupland & McClements, 1996; Velasco et al., 2008).

ω -3 PUFA including food formulations contain trace amounts of iron or are even fortified with iron (e.g., baby food, milk, clinical and sports nutrition). Metal ions (M) (such as copper and iron) are well known as catalyst of lipid oxidation even at trace levels (Frankel, 2015). Several studies connected iron to lipid oxidation (Choe et al., 2014; Guzun-Cojocararu et al., 2010; Mei, Decker, et al., 1998; Mei, McClements, et al., 1998; Nuchi et al., 2001). Artificial radical initiators such as azo compounds (A-N=N-A) can also induced lipid oxidation. These compounds decompose thermally to produce two radicals (A \cdot) and Nitrogen (**1**). A \cdot reacts with oxygen, and generate peroxy radicals (AO \cdot_2) (**2**). These radicals induce lipid oxidation by hydrogen atom abstraction (**3**) (Burini, 2007; Frankel, 2015).



The objective of our study is to develop a fast extraction method for fats that allows simultaneous measurement of oxidation level using a reference method and recording of FTIR spectra. Monitoring lipid oxidation can be done by measuring primary or secondary oxidation products. PV and CD methods quantify the content of peroxides (primary oxidation products). P-Anisidine Value (pAV) and (TBARs) are used for secondary oxidation products, mainly aldehydes. We focus on the beginning of the oxidation. Therefore, peroxides content was evaluated by measuring CD value. We then use PLSR to highlight correlations between attenuated total reflectance (ATR)-FTIR spectra and CD values. Finally, we monitor iron- or radical-induced lipid oxidation in a model o/w emulsions directly.

2. Materials and methods

Refined tuna oil was produced and supplied by ZOR (A Cargill Company, Zaandam, The Netherlands). Tuna oil was bubbled with and stored under nitrogen (headspace) in small containers (1 L) at -20°C . Hexadecyltrimethylammonium bromide (CTAB) (CAS Number 57-09-0) was used as surfactant for emulsion preparation (purity $\geq 99\%$). For oxidation initiation, ferrous sulfate heptahydrate (CAS Number 7782-63-0) and 2,2'-azobis(2-methylpropionamidine)dihydrochloride (AAPH) (CAS Number 2997-92-4) were added. The chemicals used for fat extraction and for measurement of CDs were 2,2,4-trimethylpentane (CAS Number 540-84-1), 2-propanol (CAS Number 67-63-0), and sodium chloride (CAS Number 7647-14-5). All chemicals were analytical grade and purchased from Merck Sigma-Aldrich (Munich, Germany).

2.1. Emulsion preparation and oxidation conditions

O/w emulsions were prepared using a two-stage process. First, 20% (v/v) tuna oil and 80% (v/v) buffer solution (10 mM phosphate buffer (pH = 7), 0.7% (w/v) CTAB (cetyltrimethylammonium bromide) as emulsifier) were blended three times, for 1 min each time, at 20,500 rpm using a rotor/stator homogenizer (Ultra Turrax® T25; IKA-Labortechnik, Munich, Germany). The coarse emulsion was then homogenized four times at 35 MPa using a microfluidizer (LM10; Microfluidics, Westwood, MA, USA) (Guzun-Cojocar et al., 2011). No bubbling or purging with nitrogen was done, and oxygen from the air was uncontrolled during homogenization. Twenty mL of each emulsion were transferred into 100 mL capped bottles. For radical initiation, 2 g of AAPH (10% w/v final concentration) was mixed for 10 min into 20 mL of emulsion. Then emulsions were kept at 40°C to ensure decomposition of AAPH into reactive radicals (Burini, 2007; Frankel, 2015). For iron initiation, a volume (twenty / two microliters) of sulfate iron solutions (1 M / 0.1M), were added to 20 mL of emulsion to obtain final concentrations of 10^{-3} M and 10^{-5} M iron (II) respectively, which were kept at 25°C . Samples were covered with aluminum foil to prevent light exposure. At least two repetitions of each set of samples were prepared.

2.2. Rapid fat extraction method

Measuring CD values is one of the most used methods to evaluate lipid oxidation in its early stages. However, CD value determination requires lipid extraction for complex matrices, such as o/w emulsions. For an accurate evaluation of oxidation, this extraction should be efficient and reproducible (Velasco et al., 2008).

The efficiency of the solvent extraction depends on the polarity of the lipid present compared with the polarity of the solvent. In this method, a mixture of isooctane/2-propanol (3:1) ensured a total fat extraction. Cesa et al.(2012) showed that an extraction using only a nonpolar solvent, such as hexane, not only gives very low yields, but also tends to overestimate oxidation levels: i.e., hexane can selectively extract surface fat that is most exposed to oxygen (Cesa et al., 2012). In addition, this solvent blend is safer for users than hexane–dichloromethane or chloroform–methanol mixtures (the Folch method (Folch et al., 1957)).

After adding this binary solvent mixture to the emulsions, salt was added (sodium chloride) to speed up the process of phase separation. Based on the Derjaguin–Landau–Verwey–Overbeek theory, the stability of a colloidal system is the result of an equilibrium between the electrostatic and the van der Waals interactions acting on particles (Ohshima, 2014). It is well known that adding a high concentration of salt provides a high ionic strength to the system. This variation influences the double-layer interactions on the surface of droplets, which decreases the repulsive forces between them. Once the repulsive interaction is lowered, the particles can overcome the energy barrier and collide (Adair et al., 2001). The coalescence phenomena are then faster and more efficient, which results in a clear fat separation. This method can separate lipid/water phases using small amounts of sample and organic solvents. It does not require expensive equipment, such as a centrifuge or a vacuum evaporator, and it can be done in less than 3 minutes.

Aliquots of 0.2 mL were added to 1 mL of isooctane/2-propanol (3:1) solution (Young-Je Cho et al., 2002) and 0.024 g of sodium chloride in a 5 mL plastic tube. The mixture was vortexed for 1 min and left to stand for 1 min for phase separation.

2.3. Determination of CDs

CDs are considered primary products of peroxide oxidation:



CDs were measured according to the AOCS official method Ti 1a-64 (AOCS, 2009) with some modifications. A volume of 20 - 50 μL of the upper layer was diluted in isooctane, and absorbance spectra were recorded between 200 and 300 nm using an UV-Vis spectrophotometer (UVmc $\text{\textcircled{R}}$, SAFAS, Monaco) with a data interval of 1 nm and a band path of 2 nm. Pure isooctane was used as a reference. The value of CDs was expressed in millimoles of equivalents peroxide (LH) per kilogram of oil ($\text{mmol eq LH}\cdot\text{kg}^{-1}_{\text{oil}}$) using a molar extinction coefficient of $27,000 \text{ M}^{-1}\cdot\text{cm}^{-1}$ (Lethuaut et al., 2002) at 233 nm.

2.4. Physical stability of the emulsion

The physical stability of emulsions was measured using a Turbiscan™ LAB (Formulation, Toulouse, France). The Turbiscan is equipped with a pulsed near-infrared light source ($\lambda = 880$ nm) and two synchronous detectors for transmittance (at 180°) and backscattering (at 45°), which move up and down along a cylindrical glass tube containing the sample. Data were collected every 40 μm . The light flux pattern as a function of the sample height was collected during storage. Changes in the backscattered light can reveal destabilization mechanisms such as creaming, sedimentation, flocculation, and coalescence.

2.5. FTIR measurements

A FTIR spectrometer (Model Spectrum 65; PerkinElmer, Waltham, MA, USA) coupled to an ATR accessory (ZnSe crystal) was used to measure oxidation in o/w emulsions.

Each sample (20 μL of oil-in-water emulsion, $\Phi=20\%$ v/v) was spread directly on the crystal surface and the absorbance spectrum was collected. A dry and empty ATR cell was used as a reference. The ATR spectra were averaged over 16 scans in the range of $4000\text{--}600$ cm^{-1} and recorded with a resolution of 4 cm^{-1} . All analyses were carried out at room temperature. The crystal was cleaned with ethanol and water.

2.6. Chemometrics analysis

Data were analyzed using Unscrambler® X software (version 10.5; CAMO Software, Oslo, Norway) (Esbensen, 2012). PLSR was used to show correlations between the FTIR spectra features and CD values obtained by the standard reference method.

PLSR models the relationship between a set of predictor variables (X; the FTIR spectra) and a set of responsive variables (Y; measured CD values). PLSR helps to analyze data with many noisy, collinear, and even incomplete X and Y variables (Wold et al., 2001). ATR-FTIR data presents many common artifacts related to physical states of samples (particle size, homogeneity level...) or to instrument limitations (low signal, scattering...) (Engel et al., 2013; L. C. Lee et al., 2017). Pretreatment of spectral data is crucial for such interferences. Different approaches to select pretreatment strategies can be used or combined (Engel et al., 2013). In this study, visual inspection was first done by overlapping o/w emulsions spectrums. Scatter effect and baseline shift were noticed. Therefore, descriptive analysis were applied on spectral data. This analysis provided maximum, minimum, standard deviation and others statistics parameters for each wavenumber. Large variation (standard deviation) was seen all over the spectrum. This phenomena could be a sign of scatter effect (Engel et al., 2013). Several

preprocessing tools were tested (see supplementary data A). Standard Normal Variate (SNV) followed by baseline correction were chosen.

SNV aims to subtract the spectrum mean from each spectral variable (centering spectral values) and subsequently divides that value by the standard deviation of the spectrum (scaling spectral values) (Dhanoa et al., 1994; Engel et al., 2013). This tool limited larger variations in regions of interest (listed in table 1 and related to lipid oxidation). Based on that, SNV and baseline correction were applied on raw spectral data.

Three sets of 25, 27, and 25 samples were selected for establishing calibration models to ensure the incorporation of all acceleration conditions used in this work, i.e. 10^{-3} M Fe^{2+} , 10^{-5} M Fe^{2+} and 10% AAPH (a water-soluble azo radical initiator), respectively. The coefficient of determination (R^2) and the root mean square error of calibration (RMSEC) were used to evaluate the performance of each model. To assess the feasibility of the calibration model, cross-validation was applied because of the limited number of samples. Moreover, the number of PLSR factors was chosen based on the minimum root mean square error of cross-validation (RMSECV) (Esbensen, 2012). A model was considered good when it has the higher coefficient of determination (R^2), the lowest root mean square error of calibration (RMSEC) and validation (RMSEV) and the closer RMSEC and RMSEV with the minimal number of factors (Brereton, 2006; Cebi et al., 2017; Westad & Marini, 2015).

3. Results

3.1. Changes in infrared spectra during oxidation

Before the analysis of oil oxidation kinetics, the physical stability of the emulsion was verified to ensure reproducibility of the FTIR method. During storage, the model emulsion prepared with the surfactant CTAB was fully physically stable. The FTIR spectra of the o/w emulsion (20% oil) were recorded in the range of $4000\text{--}600\text{ cm}^{-1}$. Spectral changes were similar for all oxidations conditions. Both types of initiation lead to the same oxidation products: alkyl and peroxy radicals (L^\bullet and LOO^\bullet). These reactive radicals abstract hydrogen atoms from other unsaturated fatty acids to form hydroperoxides (LOOH). Subsequently, LOOH decompose into secondary products (ketones, aldehydes, ethers and alkanes...) (Frankel, 2015). However, when radical initiator was used, a peak near 1697 cm^{-1} was noticed. This band could be attributed to -NH_2 group of AAPH (see supplementary data B). **Figure 1** shows an overlay of emulsion spectra oxidized using 10^{-3} M iron (II) over 15 days of storage in the dark with contact with air

headspace (emulsion occupied approximately one fifth of the volume of a jar closed with a screw cap) at room temperature.

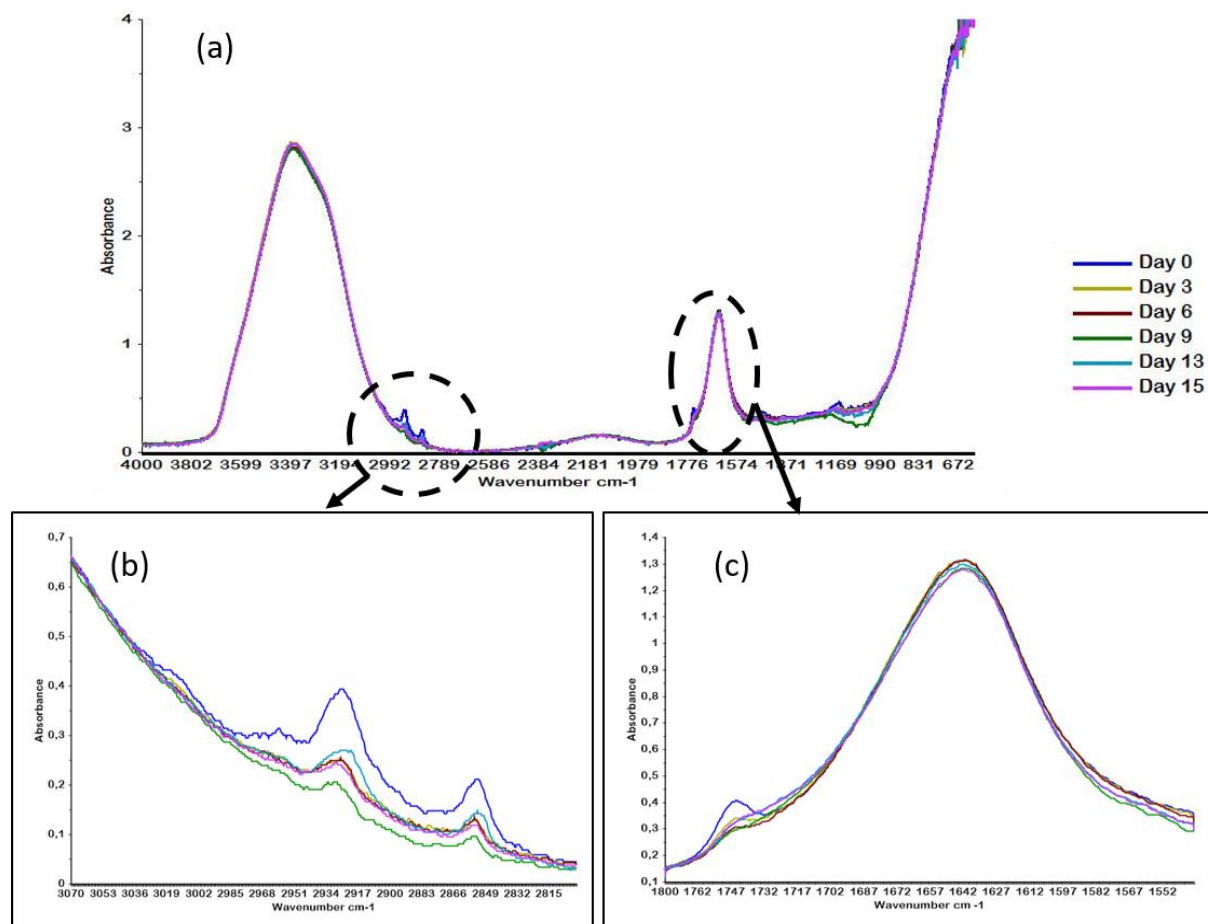


Figure 1. Infrared spectra recording of oil-in-water emulsion. (a) FTIR spectra of oil-in-water emulsions (20% fish oil) during 15 days of oxidation using 10^{-3} M iron (II) in the dark, at room temperature; (b) Zoom in at region $3070\text{--}2800\text{ cm}^{-1}$; (c) Zoom in at carbonyl band around $1800\text{--}1500\text{ cm}^{-1}$.

The major changes in the FTIR spectra are summarized in **Table 1**. The hydroxyl region spreads between $3700\text{--}3100\text{ cm}^{-1}$. It contains the stretching vibrations of OH from water, hydroperoxides (LOOH, primary products of lipid oxidation), and their breakdown products (aldehydes, alcohols, and ketones). This band remains unaltered in the first stage of oxidation. After 13 days, a slight increase in this range was noticed, which results from the formation of hydroperoxides. Belhaj et al. 2010, described the same phenomena during the thermal oxidation of salmon oil, but it was more pronounced because of the absence of huge amounts of water (BELHAJ et al., 2010). In the present work, the high water content of the emulsion (80% v/v) restricts the use of this region ($3700\text{--}3100\text{ cm}^{-1}$) to record oxidation kinetics by classical FTIR.

Figure 1b shows a weak band at 3012 cm^{-1} . The decrease of this band is associated with a decrease of the C–H stretching vibration of the *cis*-double bond (C=C) (Guillen & Cabo, 2000). The frequency of this band, as described in the literature, ranges between 3006 and 3009 cm^{-1} . The shift can be explained by the different fatty acid compositions and degrees of unsaturation of the used oil. Once lipids are oxidized, the *cis*-double bond rearranges to form a *trans*-double bond, resulting in the decrease of the band at 3012 cm^{-1} (Borchman & Sinha, 2002; Guillen & Cabo, 2000; Hayati et al., 2005). The bands at 2925 and 2852 cm^{-1} were related to asymmetric and symmetric stretching vibrations of methylene ($-\text{CH}_2$) and methyl ($-\text{CH}_3$), respectively (Cebi et al., 2017; Hayati et al., 2005; Vlachos et al., 2006).

Table 1. Major ATR-FTIR bands changing during oxidation

Wavenumber (cm^{-1})	Assignment	Changes
3700–3100	Hydroxyl region (peroxide, water)	Slight increase
3012	<i>Cis</i> -double bond $-\text{HC}=\text{CH}$ (loss)	Decrease
1747	Carbonyl group $-\text{C}=\text{O}$ (ester)	Decrease
1452	Methylene and methyl bending $-\text{CH}_2, -\text{CH}_3$ bending	Increase
1377	Methylene and methyl bending $-\text{CH}_2, -\text{CH}_3$ stretching	Increase
1161	Carbonyl group $-\text{C}-\text{O}$	Increase
968	<i>Trans</i> -double bond $-\text{HC}=\text{CH}-$ (formation)	Increase

The band near 1747 cm^{-1} (**Figure 1c**) was attributed to the stretching vibrations of the carbonyl group of triglyceride esters ($-\text{C}=\text{O}$) (Cebi et al., 2017; Guillen & Cabo, 2000; Hayati et al., 2005; Klaypradit et al., 2011). This band should increase during the oxidation process; however, this band was not found in our study. This can be explained by the fact that other bands (1725 and 1705 cm^{-1}), which are related to the formation of aldehydes and ketones, respectively, overlapped with the band at 1747 cm^{-1} and decreased its intensity as oxidation advanced. Similar changes were reported for thermal oxidation of palm kernel olein, soybean oil (Hayati et al., 2005), and corn oil (Vlachos et al., 2006). In the same region, a strong band at 1644 cm^{-1} can be identified as C–H bending vibrations of methylene, overlapping with the O–H deformation of water present in the system. It may also contain the symmetrical stretching vibrations of conjugated C=C at 1634 cm^{-1} (Hayati et al., 2005). An interpretation of the spectra near 1640 cm^{-1} regarding oxidation over time was not trivial because of overlapping peaks.

The fingerprint region at 1500–900 cm^{-1} enclosed: the CH_2 bending band at 1452 cm^{-1} , and the C–O/ CH_2 stretching and bending band at 1161 cm^{-1} (Cebi et al., 2017; Hayati et al., 2005). The intensity of these bands increased during oxidation because of the decomposition of hydroperoxides through the β -scission mechanism (Frankel, 2015; Hayati et al., 2005). The band at 1377 cm^{-1} was identified as C–H bending vibrations of methyl groups. Another important band is the one at 968 cm^{-1} , which corresponds to the C–H out-of-plane deformation vibration of *trans*-double bonds. Its frequency increases during oxidation (*cis*-double bonds of unsaturated fatty acids undergo isomerization to the *trans*-form) (Borchman & Sinha, 2002), (Cebi et al., 2017; Kim et al., 2007).

3.2. CDs as reference method

Measurement of CD values was chosen to monitor primary products of lipid oxidation. It has been privileged on PV which requires more time and solvents. During storage, all samples showed increased CD content (Figure 2).

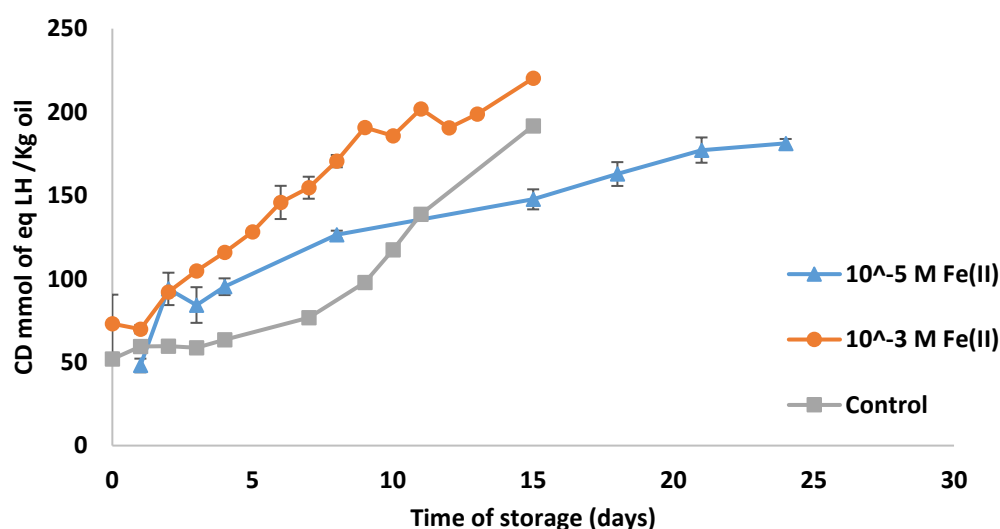
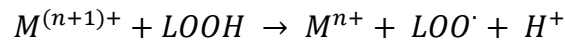
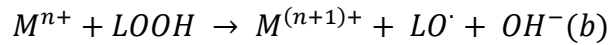


Figure 2. Changes in Conjugated diene values of 20% oil-in-water emulsions. Emulsions: (■) control (no iron added), (Δ) with 10^{-5} M Fe (II) ($n = 3 \pm \text{SD}$) and (●) 10^{-3} M Fe (II) ($n = 2 \pm \text{SD}$), were kept at room temperature.

While the induction time for control emulsions was around seven days, the emulsions with iron (II) showed a very short lag phase of one and three days for 10^{-3} and 10^{-5} M Fe^{2+} , respectively. This is closely linked to the prooxidant effect of iron on lipid oxidation. As described by Frankel, trace amounts of heavy metals accelerate the rates of lipid oxidation through two pathways (Frankel, 2015): electron transfer (a) and formation of metal–oxygen

complexes or metal–hydroperoxide complexes (M–HOOL) that catalyze autoxidation and decomposition by one electron redox reactions (b).



Even though no iron metals were added to the control emulsions, oxidation was still pursued. Actually, trace amounts of iron can be present in the oil and water used to produce the emulsion. Moreover, a small part of dioxygen in the air is not at ground state (3O_2 , O=O), but at the excited state (1O_2 , $\bullet O-O\bullet$) due to air pollution and sun light (Wayne, 1994). The 1O_2 content in the atmosphere depends on the weather (Ogawa et al., 1996). Hydroxy radicals $HO\bullet$ in urban air were also quantified (Alaghmand & Blough, 2007). This natural presence of radicals in the air explains why oils are oxidized even without adding prooxidants.

Once the initiation is completed, CDs are the primary products of oxidation. They are retained in many products after LOOH decomposition, e.g., in alcohols formed by hydrogen abstraction as well as in some scission products (Karen M. Schaich et al., 2017). The three curves tend to plateau over time. Similar results were also shown by Lethuaut et al. when sunflower oil emulsions were oxidized. This was explained by linking CD formation to oxygen consumption. In fact, the steady-state phase of CD formation was reached at the same time as a limiting value of O_2 uptake; therefore, oxygen was considered as the limiting factor (Lethuaut et al., 2002). In addition, the plateau can be related to the fact that net CD values are the result of both CDs produced and CDs converted into secondary products of oxidation.

In the samples where oxidation was induced using the radical initiator AAPH (10% w/v at 40 °C), CD formation was very fast; i.e., a lag phase of only 2 hours was recorded (supplementary data C).

3.3. Correlation between FTIR spectra and CD value

Correlation between standard oxidation measurement methods and infrared spectroscopy has been widely investigated, especially in bulk oil. Several researchers have been seeking relationships between peaks or spectral ranges and oxidation parameters (e.g., 990–940 cm^{-1} with PV for microalgae oil (Cebi et al., 2017), 3700–3100 cm^{-1} and *cis*-bond frequency near 3010 cm^{-1} with CD values and polyene index for salmon oil, marine lecithin and emulsions for their combination (BELHAJ et al., 2010), and the carbonyl region 1710–1670 cm^{-1} with TBARS in palm olein (Setiowaty & Che Man, 2003)).

However, the FTIR spectra can be very hard to interpret because of overlapping bands (as described in subsection 3.1). In addition, different oxidation products can have similar functional groups that absorb energy in the same region. One should also notice that, in our case, the presence of a huge amount of water (80% v/v) aggravates this situation.

The ability of the PLSR method to counteract these limitations was evaluated. Calibration models were calculated using the whole spectrum (4000–700 cm^{-1}) and different spectral regions such as the hydroperoxide one (3800–3070 cm^{-1} and 3070–2800 cm^{-1}), the carbonyl region (1800–1500 cm^{-1}), and the fingerprint region (1500–700 cm^{-1}). The calibration and cross-validation parameters are presented in **Table 2**.

Table 2. Calibration and cross validation results of PLS models for CD value prediction.

(R² Pearson for p-value < 0.0005)

	Regions (cm ⁻¹)	Calibration		Cross-validation			N. factors
		R ² ^a	RMSEC ^b	R ²	RMSECV ^c	Bias ^d	
AAPH	4000–700	0.955	9.304	0.832	18.778	2.16	7
	3800–2800; 1800–700	0.93	11.55	0.837	17.87	0.418	6
	3800–3070	0.884	14.918	0.763	21.169	-0.735	5
	3070–2800	0.832	17.926	0.736	24.66	0.173	4
	1800–1500	0.975	6.948	0.846	16.002	1.167	7
	1500–900	0.905	13.488	0.814	21.583	0.305	5
10⁻³M	4000–700	0.991	5.122	0.816	24.713	0.367	7
Fe²⁺	3800–2800; 1800–700	0.994	4.16	0.823	23.759	1.004	5
	3800–3070	0.996	3.292	0.655	33.374	3.281	7
	3070–2800	0.897	17.497	0.704	34.534	1.564	5
	1800–1500	0.911	16.281	0.791	24.139	1.831	5
	1500–900	0.968	9.805	0.928	18.165	1.803	5
10⁻⁵M	4000–700	0.979	5.62	0.859	14.117	-2.239	7
Fe²⁺	3800–2800; 1800–700	0.971	6.599	0.854	14.781	-2.106	6
	3800–3070	0.967	7.086	0.817	18.328	-0.707	7
	3070–2800	0.835	15.76	0.469	28.051	-2.38	6
	1800–1500	0.96	7.78	0.784	18.447	-0.93	7
	1500–900	0.975	6.175	0.814	18.752	0.101	7

^a coefficient of determination, ^b root mean square error of calibration, ^c root mean square error of cross-validation, ^d average value of difference between predicted and measured values.

In general, significant positive correlations were obtained. The coefficient of determination R^2 varied between 0.996–0.832 and 0.928–0.469 for the calibration and cross-validation models, respectively. These coefficients of determination R^2 were, in all cases, more important than the R^2 Pearson significance threshold value for p -value < 0.0005 (R^2 Pearson = 0.382). Error values ranged from 3.29 to 17.93 mmol eq LH kg⁻¹_{oil} (RMSEC) and 14–34.5 mmol eq LH kg⁻¹_{oil} (RMSECV).

When using radical initiation, values of CDs range from 63.3–240.2 mmol eq LH kg⁻¹_{oil} (mean value = 107). Models, whether calculated from the whole spectrum data or from specific data regions, provided good predictions of CD values. Indeed, coefficient of determination varied from 0.832 to 0.975, and RMSECVs ranged between 16–25.5 mmol eq LH kg⁻¹_{oil} (corresponding to 14–23.8%). The 1800–1500 cm⁻¹ range provided the best calibration model (**Figure 3a**). The same behavior was noticed for iron initiation. For the first initiation with 10⁻³ M Fe²⁺, the measured CD values ranged from 51.8–220.3 mmol eq LH kg⁻¹_{oil} (mean value = 122.9) (**Figure 3**).

When considering all the spectral ranges, the calibration model gave a R^2 of 0.991 and a RMSEC = 5.12 mmol eq LH kg⁻¹_{oil} (4.17%). The loading of factor 1 showed peaks like 3010 cm⁻¹, 1745 cm⁻¹, 1720 cm⁻¹, and 966 cm⁻¹ that are closely related to lipid oxidation (data not shown). By just taking out all variables in the range of 2800 to 1800 cm⁻¹ (where nothing changed in the spectrum during oxidation), an improvement of the calibration and prediction models was achieved.

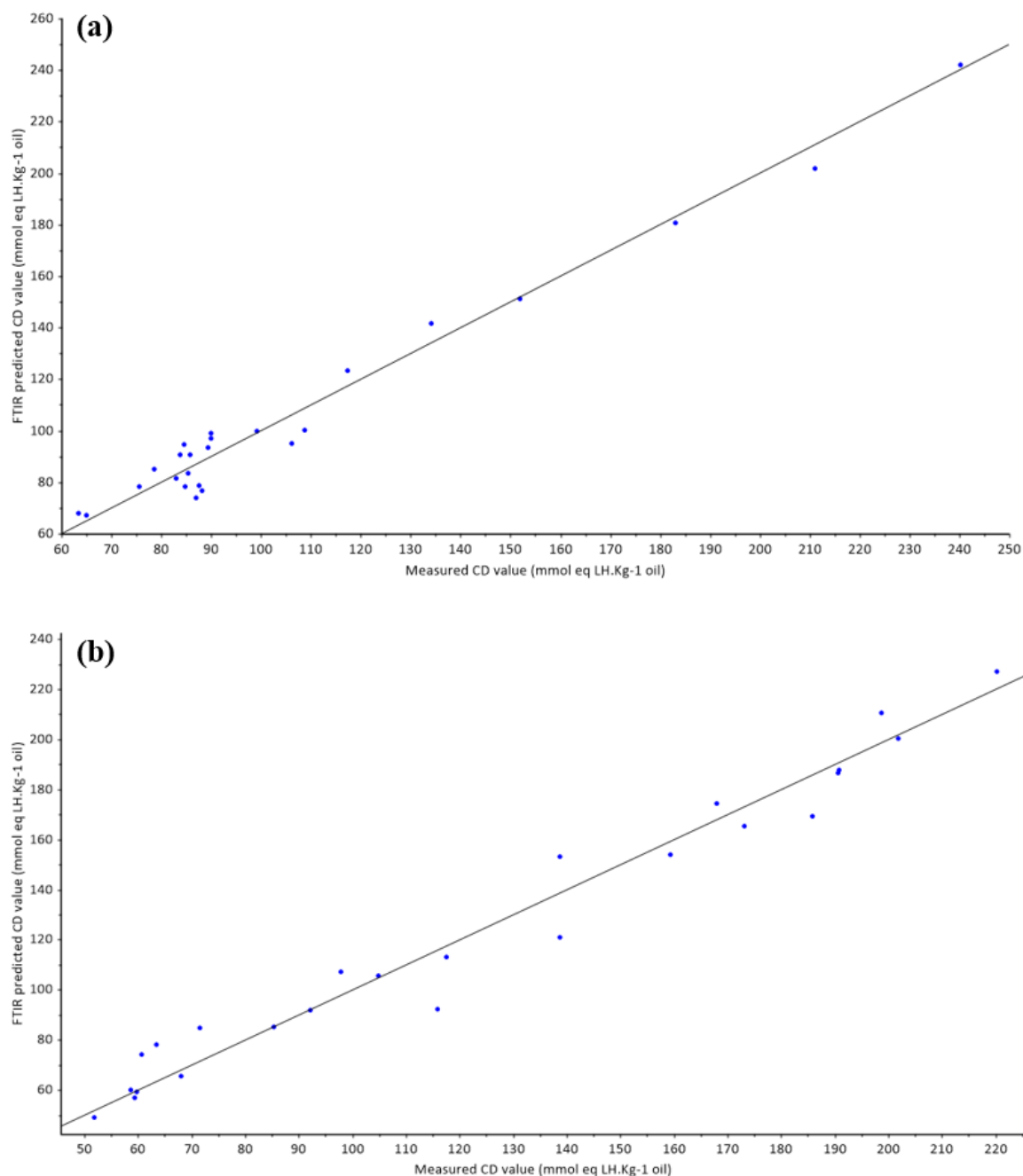


Figure 3. Calibration plot of FTIR-predicted vs. measured CD values

(a) region $1800\text{--}1500\text{ cm}^{-1}$ for radical initiation (10% AAPH) and (b) region $1500\text{--}900\text{ cm}^{-1}$ for iron (II) initiation (10^{-3} M)

The region of hydroxyl vibration ($3800\text{--}3070\text{ cm}^{-1}$) produced a good calibration model ($R^2 = 0.996$ and $\text{RMSEC} = 3.292\text{ mmol eq LH kg}^{-1}\text{ oil}$ (2.6%)), but not a good prediction model ($R^2 = 0.655$ and $\text{RMSECV} = 33.374\text{ mmol eq LH kg}^{-1}\text{ oil}$). As for the region of $3070\text{--}2800\text{ cm}^{-1}$, which contained the *cis*-double bond, the calibration and cross-validation parameters were not

satisfying. This can be simply explained by the presence of the broad band of water in this region that hides changes in the weak band at 3010 cm^{-1} . Hayati et al. stated the same problem, even though they were studying a 70% o/w emulsion (only 30% water phase) (Hayati et al., 2005).

The region of $1800\text{--}1500\text{ cm}^{-1}$ provided calibration and validation models with good R^2 , but with a considerable RMSECV of $24.139\text{ mmol eq LH kg}^{-1}_{\text{oil}}$ (19.6%). This result is acceptable considering that different bands appear in this region during oxidation (see subsection 3.1). Therefore, issues due to overlap may occur. However, the best model was the one using the fingerprint region ($1500\text{--}900\text{ cm}^{-1}$). It provided good coefficient of determination and low error (RMSEC = 8% and RMSECV = 14%) for calibration and validation models. This PLSR model uses only five factors and presents good prediction ability (bias = 1.803, or 1.46%). **Figure 3b** shows the scatter plots of measured CD values vs the predicted values from this model. This result is related, at least partly, to the presence of the *trans*-double bonds band at 968 cm^{-1} . This band was not altered by the presence of water and is already known to be the predominant prediction factor of oxidation (Cebi et al., 2017; Kim et al., 2007). Actually, *trans*-double bonds do not occur naturally in plant lipids, they are produced during oxidation (Borchman & Sinha, 2002).

For the samples where 10^{-5} M of iron (II) was added, CD values ranged from 66.8–184.6 $\text{mmol eq LH kg}^{-1}_{\text{oil}}$ (mean value = 128.1). Good correlations were found when using the whole spectral range, the $1800\text{--}1500\text{ cm}^{-1}$ region, and the fingerprint region. Once again, the use of the region $3070\text{--}2800\text{ cm}^{-1}$ resulted in models with the lowest coefficient of determination ($R^2 = 0.835$) and, importantly, a RMSECV of $28.05\text{ mmol eq LH kg}^{-1}_{\text{oil}}$.

4. Conclusion

In this work, lipid oxidation was monitored and quantified in o/w emulsions using CD values after a lipid extraction. ATR-FTIR spectroscopy combined with chemometrics tools (PLSR) allowed a rapid, easy, and accurate prediction of CD values of emulsions without any sample preparation. PLSR models were established using whole spectra ($4000\text{--}700\text{ cm}^{-1}$), the carbonyl region ($1800\text{--}1500\text{ cm}^{-1}$) and the fingerprint regions ($1500\text{--}700\text{ cm}^{-1}$). These models provided good prediction of CD values with an average error (mean of RMSECV) of less than 18%. The developed ATR-FTIR technique is cost-effective, fast, nondestructive (with a very small volume of sample is necessary), and it minimizes the use of organic solvents. Though the presence of water, it seems not necessary to use Raman-spectroscopy to monitor oil oxidation

in an emulsion. For the first time, this technique provides a good tool to predict oxidation status in complex systems such as 20% o/w emulsions—without oil extraction—so that it can be used for omega-3-enriched liquid foods. However, to assure good results, the emulsions must remain physically stable. Changes in oil droplet size may induce different interactions with light, which change the infrared spectra unrelated to oxidation events.

5. Application of ATR-FTIR on lecithin-stabilized emulsion

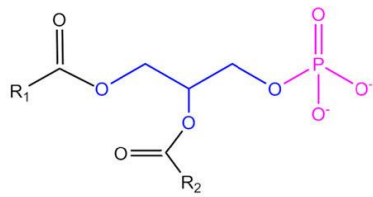
The aim of this section was to check if the analytical method could be applied to emulsions with lecithin as surfactant.

The emulsifiers used industrially to stabilize oil-in-water emulsions are usually synthetic ones. There has been an increasing consumer demand for more natural, environmentally friendly, and sustainable commercial products (McClements & Gumus, 2016). The phospholipid-based functional ingredients used as emulsifiers in commercial products are usually called lecithins. Lecithins can be isolated from numerous biological sources, with the most common being soybeans, eggs, milk, rapeseed, canola seed, cottonseed, and sunflower (Cui & Decker, 2016; McClements & Gumus, 2016). The most common phospholipids found in commercial lecithin ingredients are phosphatidylcholine (PC), phosphatidylethanolamine (PE), phosphatidylinositol (PI), and phosphatidic acid (PA), see (Erreur ! Source du renvoi introuvable.) (Cui & Decker, 2016). The hydrophilic head-groups of phospholipids are typically both anionic (PI and PA) or zwitterionic (PC and PE), with the charge depending strongly on pH. The non-polar tail groups of phospholipids usually have two fatty acids, which can vary in the number of carbon atoms and double bonds they contain. The amphiphilic character allowed usage of lecithins as surface-active agents.

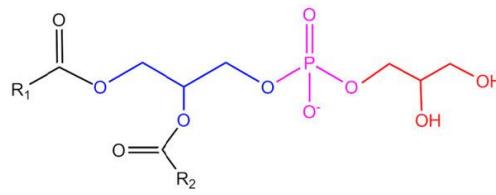
The beneficial health effects of phospholipids have been well exposed. The benefits included regulating the inflammatory reaction, e.g. arthritis, inhibiting tumor growth and metastasis, lowering cholesterol and cardiovascular risks, enhancing learning and memory, and

improving immunological functions and acting on Parkinson's disease (Canty & Zeisel, 1994; L. Liu et al., 2013; Wang et al., 2018).

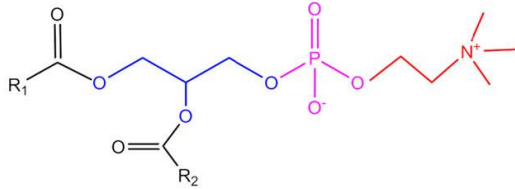
Lecithin can be a substrate for oxidation, pro-oxidant and antioxidant (Cui & Decker, 2016). Due to their insaturations, phospholipids can undergo oxidation through the radical chain reactions. The reaction is initiated in the presence of heat, light, oxygen or transition metals (such as iron). This process leads to low molecular weight compounds like aldehydes and ketones, resulting in rancidity and off-flavors. In the other hand, in bulk oil, phospholipids can form reversed micelles. These microstructures present oil-water interfaces where hydrophilic prooxidants (e.g. iron) are in close contact with oxidation substrates. Thus, the rate of oxidation increases.



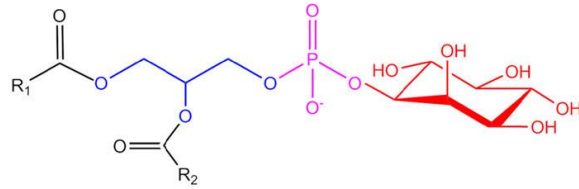
Phosphatidic acid (PA)



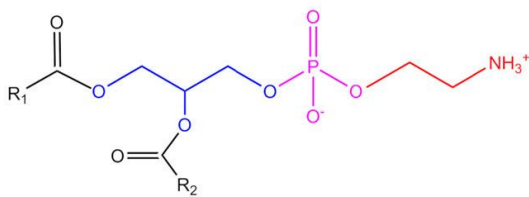
Phosphatidylglycerol (PG)



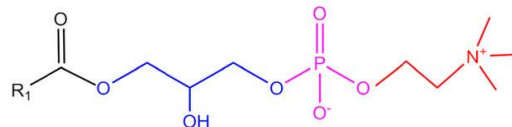
Phosphatidylcholine (PC)



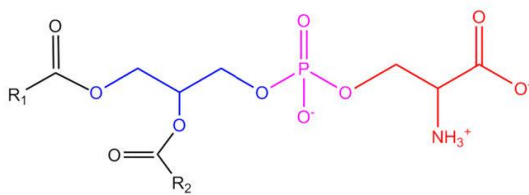
Phosphatidylinositol (PI)



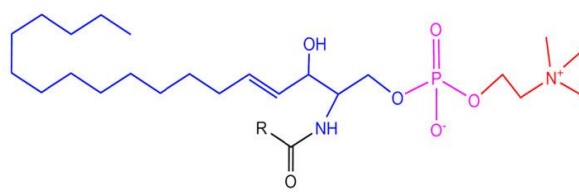
Phosphatidylethanolamine (PE)



Lysophosphatidylcholine (LPC)



Phosphatidylserine (PS)



Sphingomyelin (SPM)

Figure 4. The structures of some phospholipids (Cui & Decker, 2016)

(PA) Phosphatidic acid, (PG) Phosphatidylglycerol, (PC) Phosphatidylcholine, (PI) Phosphatidylinositol, (PE) Phosphatidylethanolamine, (LPC) Lysophosphatidylcholine, (PS) Phosphatidylserine and (SPM) Sphingomyelin

The impact of phospholipids is closely related to the system nature: homogenous, heterogeneous, tocopherols presence and content... First, it had been clearly proved that lecithin chelate iron (Choe et al., 2014). This binding capacity varies in function of phospholipids composition (different charge for PA, PS, PC and PE), and depends on pH value and iron concentration. Even though lecithin can chelate iron, but not necessarily inhibit lipid oxidation.

Actually, iron chelation to be effective on inhibiting lipid oxidation, it should ensure a decrease of iron reactivity. Some chelators, when binding to iron, increase its solubility and thus its reactivity. In addition, several authors identified phospholipids as antioxidant through synergetic effect with other antioxidants (e.g. tocopherols) (Choe et al., 2014; Doert et al., 2012; K. Samdani et al., 2018). This synergism could be due to the ability of phospholipids to form antioxidative Maillard reaction products in the presence of tocopherols, alter the physical location of tocopherols and/or regenerate tocopherols. Phospholipids such as PE have a primary amine group that can serve as a Maillard reaction substrate. Besides, carbonyls produced from the β -scission reactions of lipid oxidation (e.g. aldehydes and ketones) can provide the other substrate allowing Maillard reactions to occur. These products were known for their ability to scavenge free radicals. As both tocopherols and phospholipids have surface activity properties, their combination could influence the physical location of tocopherols as well as other primary antioxidants and then bring it into close proximity to the site of greatest oxidative stress (Cui & Decker, 2016; K. Samdani et al., 2018). Regeneration of oxidized α -tocopherol would help inhibit lipid oxidation by (1) eliminating pro-oxidative oxidized α -tocopherol and (2) re-forming antioxidative α -tocopherol (Cui & Decker, 2016). The regeneration mechanism of α -tocopherol by phospholipids such as PE and PS is presented in **Erreur ! Source du renvoi introuvable.**

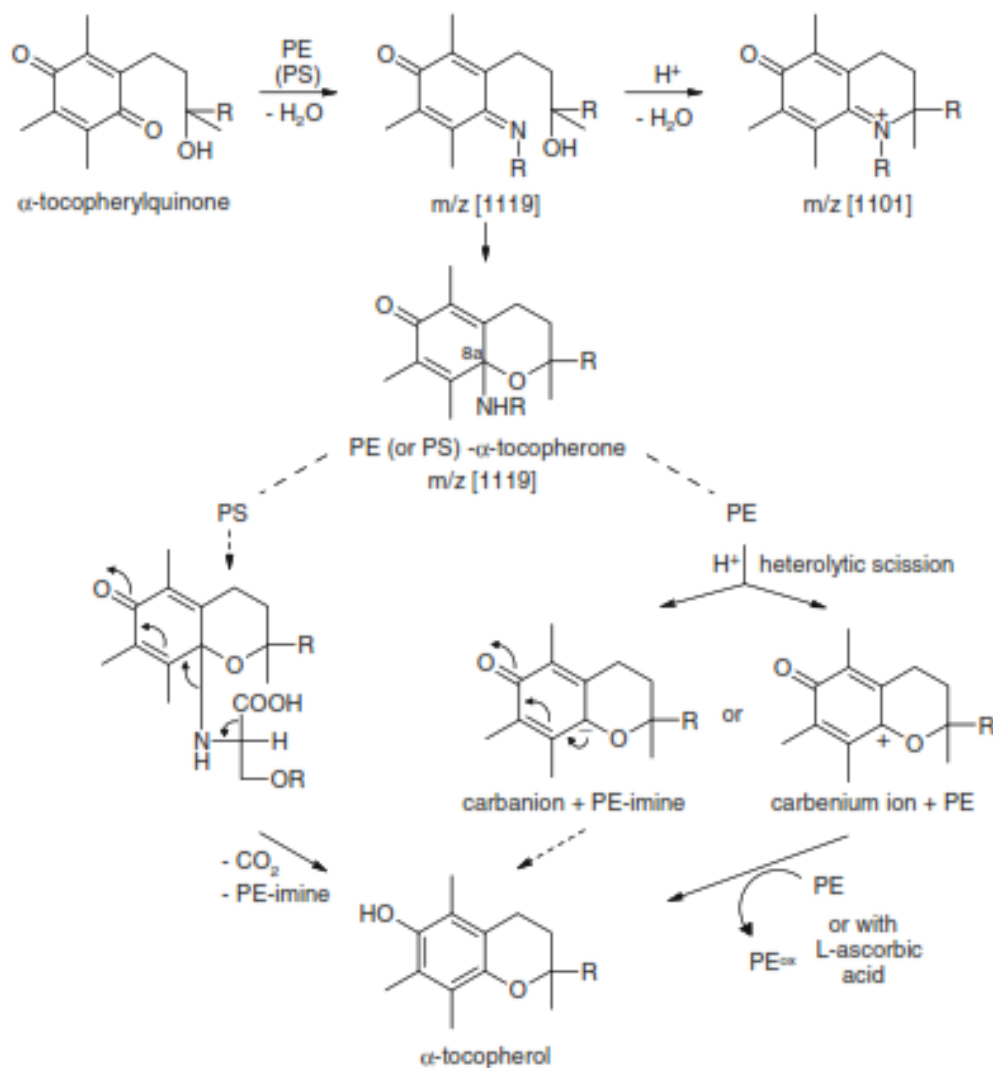


Figure 5. The regeneration mechanism of α -tocopherol by PE and PS (Doert et al., 2012)

PE or PS regenerate α -tocopheryl quinone to α -tocopherone via an amino-carbonyl reaction. The PS- α -tocopherone can be directly converted into α -tocopherol through decarboxylation. However, PS only occurs in plant lecithins in small amounts; therefore, the reaction is not of interest. On the other hand, in the reaction of PE, the heterolytic decomposition of the α -tocopherone is blocked. Nevertheless, the decomposition is catalyzed by acids. PE- α -tocopherone reacts through a heterolytic cleavage to a carbanion and PE-imine and then forms α -tocopherol by adding a proton. The other possible reaction is PE- α -tocopherone forms a

carbenium ion through the heterolytic cleavage and then it is reduced to α -tocopherol by PE or L-ascorbic acid (Doert et al., 2012).

Practically, emulsions were prepared using the same strategy detailed previously. Synthetic emulsifiers were replaced with high oleic sunflower lecithin supplied by Cargill texturizing solutions (Hamburg, Germany). Iron solution was added to a final concentration of 1 mM. Oxidation level was monitored by reference method (CD value) and ATR-FTIR spectroscopy. The CD value ranged from 65 to 180 mmol eq.LH.kg⁻¹ oil. Partial least square regression (PLSR) was used to check correlations between the two methods. Cross-validation was chosen to validate the calibration model due to the reduced number of samples. Several ranges of spectral data were tested. Parameters of formed models are summarized in **Erreur ! Source du renvoi introuvable.**

Table 3. The calibration and validation parameters of PLSR models (15 samples oxidized with 10⁻³ M of Fe²⁺)

Regions (cm ⁻¹)	Calibration		Cross Validation			Factors
	R ^{2a}	RMSEC ^b	R ²	RMSECV ^c	Bias ^d	
4000-700	0.986	4.505	0.949	9.181	1.187	5
3800-2800; 1800-700	0.998	1.675	0.98	5.704	0.839	7
3800-3070	0.984	4.69	0.945	9.52	0.125	5
3070-2800	0.942	9.54	0.911	12.625	-0.344	3
1800-1500	0.99	3.809	0.910	12.106	0.479	6
1500-700	0.997	2.022	0.898	13.35	1.433	6

^a coefficient of determination, ^b root mean square error of calibration, ^c root mean square error of cross validation, ^d average value of difference between predicted and measured values

All models were relatively good. The coefficients of determination for calibration as for cross-validation were quite higher than r^2 of Pearson for p value $< 0.05\%$ ($r^2 = 0.578$). Errors varied between 1.67 to 13.3 mmol eq LH.kg⁻¹ oil which corresponds to 1.5 - 11.9%. The best prediction model (the second model) was the one taking into account the whole spectra without the middle part where there is no variation. The loading plot of its first factor (PC1) was presented in **Erreur ! Source du renvoi introuvable..**

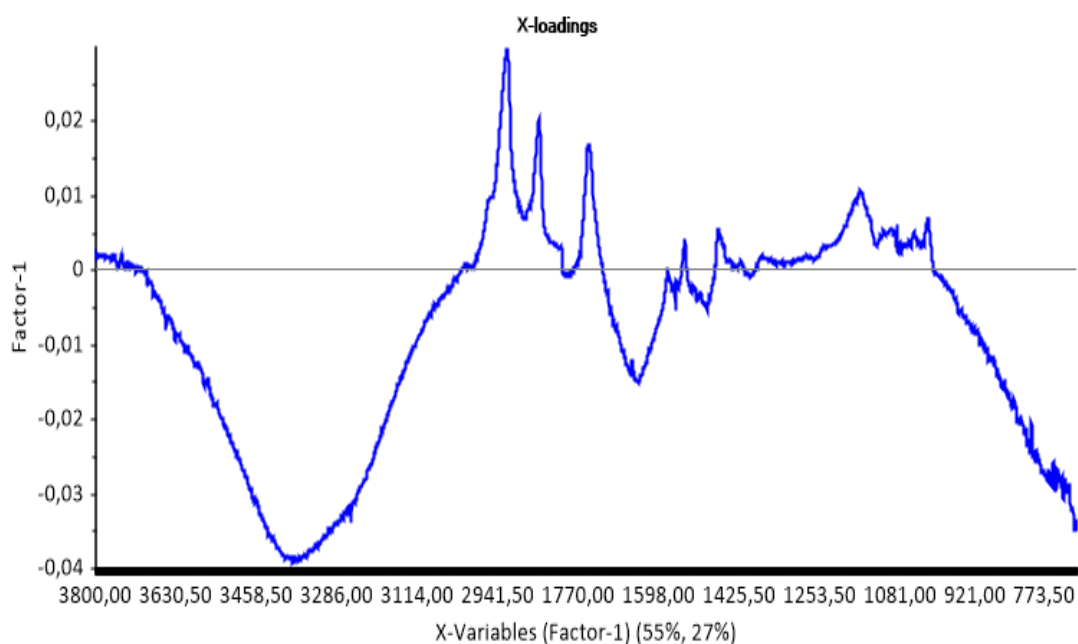


Figure 6. Loading plot of factor one from the PLSR using regions of 3800-2800 and 1800-700 cm⁻¹

It shows important variables that were identified as signs of lipid oxidation (3500, 2925, 2852, 1745 and 966 cm⁻¹...). Combining these two regions (3800-2800; 1800-700 cm⁻¹) allowed to achieve a coefficient of determination R^2 of 0.998 and the lowest error of prediction RMSECV of 5.7 mmol eq LH.kg⁻¹ oil (5% error) **Erreur ! Source du renvoi introuvable..**

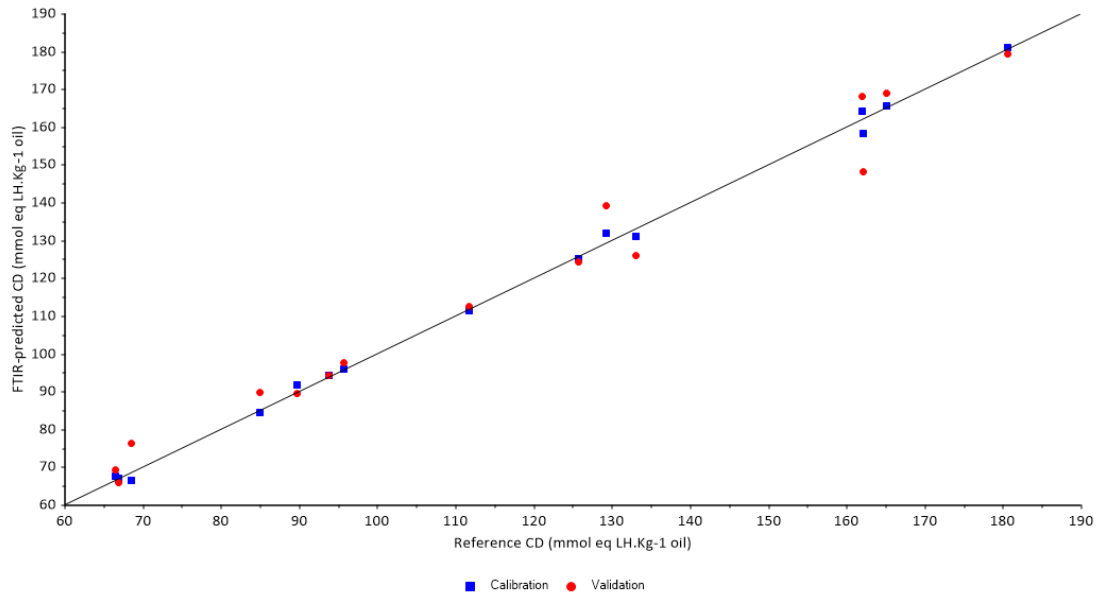


Figure 7. Relation between reference CD values and those predicted using ATR-FTIR model

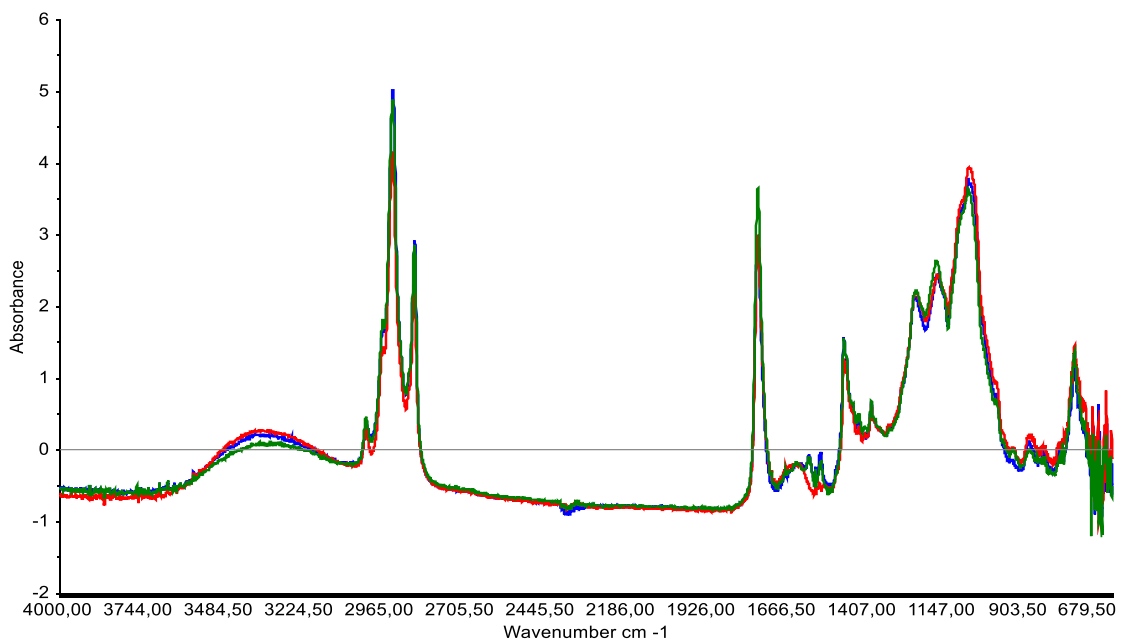


Figure 8. ATR-FTIR spectra of lecithin emulsifier (4000-600cm⁻¹)

In conclusion, despite the complex spectrum of lecithin (**Erreur ! Source du renvoi introuvable.**). FTIR spectroscopy allowed a good prediction of CD value. Thus, it can be used for monitoring lipid oxidation in such oil-in-water emulsions.

Acknowledgements

The authors gratefully acknowledge our partner Cargill, the “Fonds Européen de Développement Régional” (FEDER), and the Regional Council of Bourgogne-Franche-Comté, for their financial support.

References

- AACC. (2009). Near-Infrared Methods—Guidelines for Model Development and Maintenance. AACC International Approved Methods. <https://doi.org/10.1094/AACCIntMethod-39-00.01>
- Adair, J. H., Suvaci, E., & Sindel, J. (2001). Surface and Colloid Chemistry. In K. H. J. Buschow, R. W. Cahn, M. C. Flemings, B. Ilshner, E. J. Kramer, S. Mahajan, & P. Veyssi re (Eds.), *Encyclopedia of Materials: Science and Technology* (pp. 1–10). Elsevier. <https://doi.org/10.1016/B0-08-043152-6/01622-3>
- Alaghmand, M., & Blough, N. V. (2007). Source-Dependent Variation in Hydroxyl Radical Production by Airborne Particulate Matter. *Environmental Science & Technology*, 41(7), 2364–2370. <https://doi.org/10.1021/es061902o>
- AOCS. (2009). Spectrophotometric Determination of Conjugated Dienoic Acid- Ti 1a-64. Official Methods and Recommended Practices of the American Oil Chemists Society. <https://www.aocs.org/attain-lab-services/methods/methods/method-detail?productId=112608>
- BELHAJ, N., Arab-Tehrany, E., & Linder, M. (2010). Oxidative kinetics of salmon oil in bulk and in nanoemulsion stabilized by marine lecithin. *Process Biochemistry*, 45, 187–195. <https://doi.org/10.1016/j.procbio.2009.09.005>
- Berton-Carabin, C. C., Ropers, M.-H., & Genot, C. (2014). Lipid Oxidation in Oil-in-Water Emulsions: Involvement of the Interfacial Layer. *Comprehensive Reviews in Food Science and Food Safety*, 13(5), 945–977. <https://doi.org/10.1111/1541-4337.12097>
- Borchman, D., & Sinha, S. (2002). Determination of Products of Lipid Oxidation by Infrared Spectroscopy. In D. Armstrong (Ed.), *Oxidative Stress Biomarkers and Antioxidant Protocols* (pp. 21–28). Humana Press. <https://doi.org/10.1385/1-59259-173-6:21>
- Brereton, R. G. (2006). *Chemometrics: Data analysis for the laboratory and chemical plant* (Repr). Wiley.
- Burini, G. (2007). Development of a quantitative method for the analysis of total l-ascorbic acid in foods by high-performance liquid chromatography. *Journal of Chromatography A*, 1154(1), 97–102. <https://doi.org/10.1016/j.chroma.2007.03.013>
- Cano-Sarmiento, C., T llez-Medina, D. I., Viveros-Contreras, R., Cornejo-Maz n, M., Figueroa-Hern ndez, C. Y., Garc a-Armenta, E., Alamilla-Beltr n, L., Garc a, H. S., & Guti rrez-L pez, G.

F. (2018). Zeta Potential of Food Matrices. *Food Engineering Reviews*, 10(3), 113–138. <https://doi.org/10.1007/s12393-018-9176-z>

- Canty, D. J., & Zeisel, S. H. (1994). Lecithin and Choline in Human Health and Disease. *Nutrition Reviews*, 52(10), 327–339. <https://doi.org/10.1111/j.1753-4887.1994.tb01357.x>
- Cebi, N., Yilmaz, M. T., Sagdic, O., Yucesu, H., & Yelboga, E. (2017). Prediction of peroxide value in omega-3 rich microalgae oil by ATR-FTIR spectroscopy combined with chemometrics. *Food Chemistry*, 225(Supplement C), 188–196. <https://doi.org/10.1016/j.foodchem.2017.01.013>
- Cesa, S., Casadei, M. A., Cerreto, F., & Paolicelli, P. (2012). Influence of fat extraction methods on the peroxide value in infant formulas. *Food Research International*, 48(2), 584–591. <https://doi.org/10.1016/j.foodres.2012.06.002>
- Cheng, Z., & Li, Y. (2007). What Is Responsible for the Initiating Chemistry of Iron-Mediated Lipid Peroxidation: An Update. *Chemical Reviews*, 107(3), 748–766. <https://doi.org/10.1021/cr040077w>
- Cho, Y.-J., Alamed, J., McClements, D. J., & Decker, E. A. (2003). Ability of Chelators to Alter the Physical Location and Prooxidant Activity of Iron in Oil-in-Water Emulsions. *Journal of Food Science*, 68(6), 1952–1957. <https://doi.org/10.1111/j.1365-2621.2003.tb07000.x>
- Cho, Young-Je, McClements, D. J., & Decker, E. A. (2002). Ability of Surfactant Micelles To Alter the Physical Location and Reactivity of Iron in Oil-in-Water Emulsion. *Journal of Agricultural and Food Chemistry*, 50(20), 5704–5710. <https://doi.org/10.1021/jf020433g>
- Choe, J., Oh, B., & Choe, E. (2014). Effect of soybean lecithin on iron-catalyzed or chlorophyll-photosensitized oxidation of canola oil emulsion. *Journal of Food Science*, 79(11), C2203–2208. <https://doi.org/10.1111/1750-3841.12683>
- Codex alimentarius commission, FAO, WHO. (2017, Adopted in). Standard for fish oils, CXS 329-2017. <http://www.fao.org/fao-who-codexalimentarius>
- Coupland, J. N., & McClements, D. J. (1996). Lipid oxidation in food emulsions. *Trends in Food Science & Technology*, 7(3), 83–91. [https://doi.org/10.1016/0924-2244\(96\)81302-1](https://doi.org/10.1016/0924-2244(96)81302-1)
- Cui, L., & Decker, E. A. (2016). Phospholipids in foods: Prooxidants or antioxidants? *Journal of the Science of Food and Agriculture*, 96(1), 18–31. <https://doi.org/10.1002/jsfa.7320>
- Daoud, S., Bou-maroun, E., Dujourdy, L., Waschatko, G., Billecke, N., & Cayot, P. (2019). Fast and direct analysis of oxidation levels of oil-in-water emulsions using ATR-FTIR. *Food Chemistry*, 293, 307–314. <https://doi.org/10.1016/j.foodchem.2019.05.005>
- Dhanoa, M., Lister, S., Sanderson, R., & Barnes, R. J. (1994). The link between Multiplicative Scatter Correction (MSC) and Standard Normal Variate (SNV) transformations of NIR spectra. *Journal of Near Infrared Spectroscopy*, 2, 43–47. <https://doi.org/10.1255/jnirs.30>
- Doert, M., Jaworska, K., Moersel, J.-T., & Kroh, L. W. (2012). Synergistic effect of lecithins for tocopherols: Lecithin-based regeneration of α -tocopherol. *European Food Research and Technology*, 235(5), 915–928. <https://doi.org/10.1007/s00217-012-1815-7>
- EFSA. (2014). Scientific Opinion on the substantiation of a health claim related to DHA and contribution to normal brain development pursuant to Article 14 of Regulation (EC) No 1924/2006. *EFSA Journal*, 12(10), 3840. <https://doi.org/10.2903/j.efsa.2014.3840>
- Engel, J., Gerretzen, J., Szymańska, E., Jansen, J. J., Downey, G., Blanchet, L., & Buydens, L. M. C. (2013). Breaking with trends in pre-processing? *TrAC Trends in Analytical Chemistry*, 50, 96–106. <https://doi.org/10.1016/j.trac.2013.04.015>
- Engelmann, M. D. (2003). Variability of the Fenton reaction characteristics of the EDTA, DTPA, and citrate complexes of iron. *BioMetals*, 16(4), 519–527. <https://doi.org/10.1023/A:1023480617038>
- Esbensen, K. H. (2012). *Multivariate data analysis - in practice: An introduction to multivariate data analysis and experimental design* (5th ed., repr). CAMO.
- Ferreira, C. M. H., Pinto, I. S. S., Soares, E. V., & Soares, H. M. V. M. (2015). (Un)suitability of the use of pH buffers in biological, biochemical and environmental studies and their

interaction with metal ions – a review. *RSC Advances*, 5(39), 30989–31003.
<https://doi.org/10.1039/C4RA15453C>

- Folch, J., Lees, M., & Sloane Stanley, G. H. (1957). A simple method for the isolation and purification of total lipides from animal tissues. *The Journal of Biological Chemistry*, 226(1), 497–509.
- Francis, A. J., & Dodge, C. J. (1993). Influence of Complex Structure on the Biodegradation of Iron-Citrate Complexes. *Applied and Environmental Microbiology*, 59(1), 109–113.
<https://doi.org/10.1128/AEM.59.1.109-113.1993>
- Frankel, E. N. (2015). *Lipid Oxidation* (Second edition). Woodhead Publishing.
- Fukuzawa, K. (2008). Dynamics of lipid peroxidation and antioxidion of alpha-tocopherol in membranes. *Journal of Nutritional Science and Vitaminology*, 54(4), 273–285.
- Fukuzawa, K., & Fujii, T. (1992). Peroxide dependent and independent lipid peroxidation: Site-specific mechanisms of initiation by chelated iron and inhibition by α -tocopherol. *Lipids*, 27(3), 227–233. <https://doi.org/10.1007/BF02536183>
- Fukuzawa, K., Kishikawa, K., Tadokoro, T., Tokumura, A., Tsukatani, H., & Gebicki, J. M. (1988). The effects of α -tocopherol on site-specific lipid peroxidation induced by iron in charged micelles. *Archives of Biochemistry and Biophysics*, 260(1), 153–160.
[https://doi.org/10.1016/0003-9861\(88\)90436-5](https://doi.org/10.1016/0003-9861(88)90436-5)
- Gliszczyńska-Świątło, A., & Sikorska, E. (2004). Simple reversed-phase liquid chromatography method for determination of tocopherols in edible plant oils. *Journal of Chromatography A*, 1048(2), 195–198. <https://doi.org/10.1016/j.chroma.2004.07.051>
- Guillen, M., & Cabo, N. (2000). Some of the most significant changes in the Fourier transform infrared spectra of edible oils under oxidative conditions. *Journal of the Science of Food and Agriculture*, 80, 2028–2036. [https://doi.org/10.1002/1097-0010\(200011\)80:14<2028::AID-JSFA713>3.0.CO;2-4](https://doi.org/10.1002/1097-0010(200011)80:14<2028::AID-JSFA713>3.0.CO;2-4)
- Guzun-Cojocar, T., Cayot, P., Loupiac, C., & Cases, E. (2010). Effect of iron chelates on oil–water interface, stabilized by milk proteins: The role of phosphate groups and pH. Prediction of iron transfer from aqueous phase toward fat globule surface by changes of interfacial properties. *Food Hydrocolloids*, 24(4), 364–373.
<https://doi.org/10.1016/j.foodhyd.2009.11.002>
- Guzun-Cojocar, T., Koev, C., Yordanov, M., Karbowski, T., Cases, E., & Cayot, P. (2011). Oxidative stability of oil-in-water emulsions containing iron chelates: Transfer of iron from chelates to milk proteins at interface. *Food Chemistry*, 125(2), 326–333.
<https://doi.org/10.1016/j.foodchem.2010.08.004>
- Hayati, I. N., Man, Y. B. C., Tan, C. P., & Aini, I. N. (2005). Monitoring peroxide value in oxidized emulsions by Fourier transform infrared spectroscopy. *European Journal of Lipid Science and Technology*, 107(12), 886–895. <https://doi.org/10.1002/ejlt.200500241>
- He, K. (2009). Fish, Long-Chain Omega-3 Polyunsaturated Fatty Acids and Prevention of Cardiovascular Disease—Eat Fish or Take Fish Oil Supplement? *Progress in Cardiovascular Diseases*, 52(2), 95–114. <https://doi.org/10.1016/j.pcad.2009.06.003>
- Hoan, P. T., & Son, T. K. (2018). Tra Catfish Oil Production: Phospholipid Removal Using Citric Acid and Bleaching Using Activated Carbon. 2018 4th International Conference on Green Technology and Sustainable Development (GTSD), 528–532.
<https://doi.org/10.1109/GTSD.2018.8595528>
- K. Samdani, G., McClements, D., & A. Decker, E. (2018). Impact of Phospholipids and Tocopherols on the Oxidative Stability of Soybean Oil-in-Water Emulsions. *Journal of Agricultural and Food Chemistry*. <https://doi.org/10.1021/acs.jafc.8b00677>
- Kim, Y., Himmelsbach, D. S., & Kays, S. E. (2007). ATR-Fourier transform mid-infrared spectroscopy for determination of trans fatty acids in ground cereal products without oil extraction. *Journal of Agricultural and Food Chemistry*, 55(11), 4327–4333.
<https://doi.org/10.1021/jf063729l>

- Klaypradit, W., Kerdpi boon, S., & Singh, R. (2011). Application of Artificial Neural Networks to Predict the Oxidation of Menhaden Fish Oil Obtained from Fourier Transform Infrared Spectroscopy Method. *Food and Bioprocess Technology*, 4, 475–480. <https://doi.org/10.1007/s11947-010-0386-5>
- Königsberger, L.-C., Königsberger, E., May, P. M., & Hefter, G. T. (2000). Complexation of iron(III) and iron(II) by citrate. Implications for iron speciation in blood plasma. *Journal of Inorganic Biochemistry*, 78(3), 175–184. [https://doi.org/10.1016/S0162-0134\(99\)00222-6](https://doi.org/10.1016/S0162-0134(99)00222-6)
- Kristinova, V., Aaneby, J., Mozuraityte, R., Storrø, I., & Rustad, T. (2014). The effect of dietary antioxidants on iron-mediated lipid peroxidation in marine emulsions studied by measurement of dissolved oxygen consumption. *European Journal of Lipid Science and Technology*, 116(7), 857–871. <https://doi.org/10.1002/ejlt.201400011>
- Laguerre, M., Bily, A., Roller, M., & Birtić, S. (2017). Mass Transport Phenomena in Lipid Oxidation and Antioxidation. *Annual Review of Food Science and Technology*, 8(1), 391–411. <https://doi.org/10.1146/annurev-food-030216-025812>
- Lee, L. C., Liong, C.-Y., & Jemain, A. A. (2017). A contemporary review on Data Preprocessing (DP) practice strategy in ATR-FTIR spectrum. *Chemometrics and Intelligent Laboratory Systems*, 163, 64–75. <https://doi.org/10.1016/j.chemolab.2017.02.008>
- Lee, Y.-M., Hong, S., Morimoto, Y., Shin, W., Fukuzumi, S., & Nam, W. (2010). Dioxygen Activation by a Non-Heme Iron(II) Complex: Formation of an Iron(IV)–Oxo Complex via C–H Activation by a Putative Iron(III)–Superoxo Species. *Journal of the American Chemical Society*, 132(31), 10668–10670. <https://doi.org/10.1021/ja103903c>
- Lerma-García, M. J., Simó-Alfonso, E. F., Bendini, A., & Cerretani, L. (2011). Rapid evaluation of oxidised fatty acid concentration in virgin olive oil using Fourier-transform infrared spectroscopy and multiple linear regression. *Food Chemistry*, 124(2), 679–684. <https://doi.org/10.1016/j.foodchem.2010.06.054>
- Let, M. B., Jacobsen, C., Frankel, E. N., & Meyer, A. S. (2003). Oxidative flavour deterioration of fish oil enriched milk. *European Journal of Lipid Science and Technology*, 105(9), 518–528. <https://doi.org/10.1002/ejlt.200300821>
- Lethuaut, L., Métro, F., & Genot, C. (2002). Effect of droplet size on lipid oxidation rates of oil-in-water emulsions stabilized by protein. *JAOCs, Journal of the American Oil Chemists' Society*, 79, 425–430. <https://doi.org/10.1007/s11746-002-0500-z>
- Liao, H., Zhu, M., & Chen, Y. (2020). 4-Hydroxy-2-nonenal in food products: A review of the toxicity, occurrence, mitigation strategies and analysis methods. *Trends in Food Science & Technology*, 96, 188–198. <https://doi.org/10.1016/j.tifs.2019.12.011>
- Liu, J., Guo, Y., Li, X., Si, T., McClements, D. J., & Ma, C. (2019). Effects of Chelating Agents and Salts on Interfacial Properties and Lipid Oxidation in Oil-in-Water Emulsions. *Journal of Agricultural and Food Chemistry*, acs.jafc.8b05867. <https://doi.org/10.1021/acs.jafc.8b05867>
- Liu, L., Waters, D. L. E., Rose, T. J., Bao, J., & King, G. J. (2013). Phospholipids in rice: Significance in grain quality and health benefits: A review. *Food Chemistry*, 139(1), 1133–1145. <https://doi.org/10.1016/j.foodchem.2012.12.046>
- Long, E. K., & Picklo, M. J. (2010). Trans-4-hydroxy-2-hexenal, a product of n-3 fatty acid peroxidation: Make some room HNE.... *Free Radical Biology and Medicine*, 49(1), 1–8. <https://doi.org/10.1016/j.freeradbiomed.2010.03.015>
- Mao, Y., Pham, A. N., Rose, A. L., & Waite, T. D. (2011). Influence of phosphate on the oxidation kinetics of nanomolar Fe(II) in aqueous solution at circumneutral pH. *Geochimica et Cosmochimica Acta*, 75(16), 4601–4610. <https://doi.org/10.1016/j.gca.2011.05.031>
- Martínez-Navarrete, N., Camacho, M. M., Martínez-Lahuerta, J., Martínez-Monzó, J., & Fito, P. (2002). Iron deficiency and iron fortified foods—A review. *Food Research International*, 35(2), 225–231. [https://doi.org/10.1016/S0963-9969\(01\)00189-2](https://doi.org/10.1016/S0963-9969(01)00189-2)
- McClements, D. J., & Gumus, C. E. (2016). Natural emulsifiers — Biosurfactants, phospholipids, biopolymers, and colloidal particles: Molecular and physicochemical basis of functional

performance. *Advances in Colloid and Interface Science*, 234, 3–26.
<https://doi.org/10.1016/j.cis.2016.03.002>

- McDonald, R. E., & Hultin, H. O. (1987). Some Characteristics of the Enzymic Lipid Peroxidation System in the Microsomal Fraction of Flounder Skeletal Muscle. *Journal of Food Science*, 52(1), 15–21. <https://doi.org/10.1111/j.1365-2621.1987.tb13964.x>
- Mei, L., Decker, E. A., & McClements, D. J. (1998). Evidence of Iron Association with Emulsion Droplets and Its Impact on Lipid Oxidation. *Journal of Agricultural and Food Chemistry*, 46(12), 5072–5077. <https://doi.org/10.1021/jf9806661>
- Mei, L., McClements, D. J., Wu, J., & Decker, E. A. (1998). Iron-catalyzed lipid oxidation in emulsion as affected by surfactant, pH and NaCl. *Food Chemistry*, 61(3), 307–312. [https://doi.org/10.1016/S0308-8146\(97\)00058-7](https://doi.org/10.1016/S0308-8146(97)00058-7)
- Nalur, S., & Decker, E. A. (1994). Rapid, sensitive, iron-based spectrophotometric methods for determination of peroxide values of food lipids. *Journal of AOAC International*, 77, 421–424.
- Nazir, N., Diana, A., & Sayuti, K. (2017). Physicochemical and Fatty Acid Profile of Fish Oil from Head of Tuna (*Thunnus albacares*) Extracted from Various Extraction Method. *International Journal on Advanced Science, Engineering and Information Technology*, 7(2), 709. <https://doi.org/10.18517/ijaseit.7.2.2339>
- Nuchi, C. D., McClements, D. J., & Decker, E. A. (2001). Impact of tween 20 hydroperoxides and iron on the oxidation of methyl linoleate and salmon oil dispersions. *Journal of Agricultural and Food Chemistry*, 49(10), 4912–4916.
- Ogawa, S., Shimazaki, R., Soejima, A., Takamura, E., Hanasaki, Y., & Fukui, S. (1996). Diurnal changes of singlet oxygen like oxidants concentration in polluted ambient air. *Chemosphere*, 32(9), 1823–1832. [https://doi.org/10.1016/0045-6535\(96\)00075-6](https://doi.org/10.1016/0045-6535(96)00075-6)
- Ohshima, H. (2014). Chapter 1—Interaction of colloidal particles. In H. Ohshima & K. Makino (Eds.), *Colloid and Interface Science in Pharmaceutical Research and Development* (pp. 1–28). Elsevier. <https://doi.org/10.1016/B978-0-444-62614-1.00001-6>
- Pham, A. N., & Waite, T. D. (2008). Oxygenation of Fe(II) in the Presence of Citrate in Aqueous Solutions at pH 6.0–8.0 and 25 °C: Interpretation from an Fe(II)/Citrate Speciation Perspective. *The Journal of Physical Chemistry A*, 112(4), 643–651. <https://doi.org/10.1021/jp077219l>
- Qian, S. Y., & Buettner, G. R. (1999). Iron and dioxygen chemistry is an important route to initiation of biological free radical oxidations: An electron paramagnetic resonance spin trapping study. *Free Radical Biology and Medicine*, 26(11), 1447–1456. [https://doi.org/10.1016/S0891-5849\(99\)00002-7](https://doi.org/10.1016/S0891-5849(99)00002-7)
- Rao, T. N. (2018). Validation of Analytical Methods. In M. T. Stauffer (Ed.), *Calibration and Validation of Analytical Methods—A Sampling of Current Approaches*. InTech. <https://doi.org/10.5772/intechopen.72087>
- Raudsepp, P., Brüggemann, D. A., Lenferink, A., Otto, C., & Andersen, M. L. (2014). Oxidative stabilization of mixed mayonnaises made with linseed oil and saturated medium-chain triglyceride oil. *Food Chemistry*, 152, 378–385. <https://doi.org/10.1016/j.foodchem.2013.11.141>
- Schaich, K. M. (1992). Metals and lipid oxidation. Contemporary issues. *Lipids*, 27(3), 209–218. <https://doi.org/10.1007/BF02536181>
- Schaich, Karen M., Xie, J., & Bogusz, B. A. (2017). Thinking outside the classical chain reaction box of lipid oxidation: Evidence for alternate pathways and the importance of epoxides. *Lipid Technology*, 29(9–10), 91–96. <https://doi.org/10.1002/lite.201700025>
- Seraghni, N., Belattar, S., Mameri, Y., Debbache, N., & Sehili, T. (2012). Fe(III)-Citrate-Complex-Induced Photooxidation of 3-Methylphenol in Aqueous Solution. *International Journal of Photoenergy*, 2012, 1–10. <https://doi.org/10.1155/2012/630425>
- Setiowaty, G., & Che Man, Y. B. (2003). A rapid Fourier transform infrared spectroscopic method for the determination of 2-TBARS in palm olein. *Food Chemistry*, 81(1), 147–154. [https://doi.org/10.1016/S0308-8146\(02\)00396-5](https://doi.org/10.1016/S0308-8146(02)00396-5)

- Sørensen, A.-D. M., Haahr, A.-M., Becker, E. M., Skibsted, L. H., Bergenståhl, B., Nilsson, L., & Jacobsen, C. (2008). Interactions between Iron, Phenolic Compounds, Emulsifiers, and pH in Omega-3-Enriched Oil-in-Water Emulsions. *Journal of Agricultural and Food Chemistry*, 56(5), 1740–1750. <https://doi.org/10.1021/jf072946z>
- Stark, K. D., Van Elswyk, M. E., Higgins, M. R., Weatherford, C. A., & Salem, N. (2016). Global survey of the omega-3 fatty acids, docosahexaenoic acid and eicosapentaenoic acid in the blood stream of healthy adults. *Progress in Lipid Research*, 63, 132–152. <https://doi.org/10.1016/j.plipres.2016.05.001>
- Suseno, S. H., Saraswati, Hayati, S., & Izaki, A. F. (2014). Fatty Acid Composition of Some Potential Fish Oil from Production Centers in Indonesia. *Oriental Journal of Chemistry*, 30(3), 975–980.
- Velasco, J., Marmesat Rodas, S., Holgado, F., Márquez-Ruiz, G., & Dobarganes, M. (2008). Influence of two lipid extraction procedures on the peroxide value in powdered infant formulas. *European Food Research and Technology*, 226, 1159–1166. <https://doi.org/10.1007/s00217-007-0645-5>
- Vlachos, N., Skopelitis, Y., Psaroudaki, M., Konstantinidou, V., Chatzilazarou, A., & Tegou, E. (2006). Applications of Fourier transform-infrared spectroscopy to edible oils. *Analytica Chimica Acta*, 573–574, 459–465. <https://doi.org/10.1016/j.aca.2006.05.034>
- Walker, R., Decker, E. A., & McClements, D. J. (2015). Development of food-grade nanoemulsions and emulsions for delivery of omega-3 fatty acids: Opportunities and obstacles in the food industry. *Food & Function*, 6(1), 42–55. <https://doi.org/10.1039/c4fo00723a>
- Wang, C., Wang, D., Xu, J., Yanagita, T., Xue, C., Zhang, T., & Wang, Y. (2018). DHA enriched phospholipids with different polar groups (PC and PS) had different improvements on MPTP-induced mice with Parkinson's disease. *Journal of Functional Foods*, 45, 417–426. <https://doi.org/10.1016/j.jff.2018.04.017>
- Wayne, R. P. (1994). Singlet oxygen in the environmental sciences. *Research on Chemical Intermediates*, 20(3), 395–422. <https://doi.org/10.1163/156856794X00397>
- Westad, F., & Marini, F. (2015). Validation of chemometric models – A tutorial. *Analytica Chimica Acta*, 893, 14–24. <https://doi.org/10.1016/j.aca.2015.06.056>
- Wold, S., Sjöström, M., & Eriksson, L. (2001). PLS-regression: A basic tool of chemometrics. *Chemometrics and Intelligent Laboratory Systems*, 58(2), 109–130. [https://doi.org/10.1016/S0169-7439\(01\)00155-1](https://doi.org/10.1016/S0169-7439(01)00155-1)
- Ye, A., Cui, J., Taneja, A., Zhu, X., & Singh, H. (2009). Evaluation of processed cheese fortified with fish oil emulsion. *Food Research International*, 42(8), 1093–1098. <https://doi.org/10.1016/j.foodres.2009.05.006>
- Yin, D., Lingnert, H., Ekstrand, B., & Brunk, U. T. (1992). Fenton reagents may not initiate lipid peroxidation in an emulsified linoleic acid model system. *Free Radical Biology and Medicine*, 13(5), 543–556. [https://doi.org/10.1016/0891-5849\(92\)90149-B](https://doi.org/10.1016/0891-5849(92)90149-B)